Thermal conductivity of diamond nanowires from first principles

Wu Li,[1,*] Natalio Mingo,[1,†] L. Lindsay,[2] D. A. Broido,[3] D. A. Stewart,[4] and N. A. Katcho[1]
[1]*CEA-Grenoble, 17 Rue des Martyrs, Grenoble 38000, France*
[2]*Naval Research Laboratory, Washington, D.C. 20375, USA*
[3]*Department of Physics, Boston College, Chestnut Hill, Massachusetts 02467, USA*
[4]*Cornell Nanoscale Facility, Cornell University, Ithaca, New York 14853, USA*
(Received 23 March 2012; revised manuscript received 9 May 2012; published 17 May 2012)

Using *ab initio* calculations we have investigated the thermal conductivity (κ) of diamond nanowires, unveiling unusual features unique to this system. In sharp contrast with Si, $\kappa(T)$ of diamond nanowires as thick as 400 nm still increase monotonically with temperature up to 300 K, and room-temperature size effects are stronger than for Si. A marked dependence of κ on the crystallographic orientation is predicted, which is apparent even at room temperature. [001] growth direction always possesses the largest κ in diamond nanowires. The predicted features point to a potential use of diamond nanowires for the precise control of thermal flow in nanoscale devices.

DOI: 10.1103/PhysRevB.85.195436 PACS number(s): 66.70.Df, 63.22.Gh

I. INTRODUCTION

Recent advances in nanofabrication and characterization techniques have made it possible to study the thermal conduction properties of very small systems, notably nanowires (NWs). The synthesis of diamond NWs eluded researchers for a long time, and they were only successfully produced recently.[1] Given the exceptional thermal conduction properties of bulk diamond, and the importance of heat dissipation in nanoscale devices, it is crucial to investigate the thermal conductivity of this new system, and to compare it with other NWs of the group IV family, Si. Due to their novelty, no experimental measurements of diamond NWs have yet been reported.

Theoretically, numerous studies of the thermal conductivity of group IV semiconductor NWs have been published in recent years.[2–11] However, the main problem that stands in the way to interpret them is the large number of approximations, assumptions, and adjustable parameters employed in all investigations to date. For any calculation, there were always the questions of "how much does the choice of interatomic potential, or the use of Mathiessen's approximation, or the choice of anharmonic scattering parameters, affect the results?" In this paper, we have developed an approach which takes an important step forward in eliminating many of these issues: we obtain κ from the numerical solution to the well-defined linearized *ab initio* Peierls-Boltzmann phonon transport equation (PBTE) as originally formulated by Peierls,[12–14] without any adjustable parameters or empirical potentials. We do not resort to the Mathiessen rule, but develop a more accurate approximation, which becomes exact in the cases where the bulk can be described by the relaxation-time approximation only. All the quantities for the system are obtained atomistically from first-principles density functional theory. The PBTE is solved iteratively, beyond the relaxation-time approximation. We have investigated cylindrical NWs with diameters above 10 nm, in the temperature range of 100–1000 K, in the [001], [011], and [111] crystallographic orientations. In what follows we present the method of calculation and results. Despite some similarities with Si, there are striking differences between the two systems. The most remarkable are (1) size affects κ more significantly in diamond than Si. For instance, at 200 nm, the room-temperature κ of diamond NWs is reduced to 25% of the bulk value, compared with 43% for Si NWs. (2) A large orientation dependence should be observable in diamond NWs already at room temperature, whereas the degree of anisotropy is generally smaller in Si NWs. (3) [001] crystallographic direction always possesses the largest κ in diamond NWs, while the direction that has the largest κ in Si NWs depends on the diameter and the temperature. These differences between diamond and Si NWs imply that it should be easier to investigate the former experimentally. They also suggest that, due to a greater tunability at larger thicknesses and higher temperatures, diamond NWs might be well suited for heat management applications in nanoscale devices.

II. PEIERLS-BOLTZMANN PHONON TRANSPORT EQUATION

Previously we have presented the *ab initio* formulation of the PBTE for bulk materials.[15–17] The case of NWs is complicated by the fact that the distribution function $f_{\mathbf{r},\lambda} = f_0(\omega_\lambda) + g_{\mathbf{r},\lambda}$ is space dependent, where λ stands for the phonon branch index and wave vector, $\lambda \equiv (\alpha, \mathbf{q})$, and $f_0(\omega_\lambda)$ is the Bose-Einstein distribution depending on the phonon frequency ω_λ. Expressing $g_{\mathbf{r},\lambda}$ in terms of phonon lifetime $\tau_{\mathbf{r},\lambda}$ defined as $g_{\mathbf{r},\lambda} = -\frac{dT}{dz} v_\lambda^z \frac{df_0}{dT} \tau_{\mathbf{r},\lambda}$, where the temperature gradient and the axes of NWs are taken along the z direction, and v_λ^z is the z component of the group velocity, the PBTE can be written as

$$1 = \left(\tau_\lambda^0\right)^{-1} \tau_{\mathbf{r},\lambda} - \Delta_{\mathbf{r},\lambda} + \mathbf{v}_\lambda \cdot \nabla \tau_{\mathbf{r},\lambda}, \tag{1}$$

where

$$\Delta_{\mathbf{r},\lambda} \equiv \sum_{\lambda'\lambda''}^{+} \Gamma^{+}_{\lambda\lambda'\lambda''} (\xi_{\lambda\lambda''} \tau_{\mathbf{r},\lambda''} - \xi_{\lambda\lambda'} \tau_{\mathbf{r},\lambda'}) + \sum_{\lambda'\lambda''}^{-} \frac{1}{2} \Gamma^{-}_{\lambda\lambda'\lambda''} (\xi_{\lambda\lambda''} \tau_{\mathbf{r},\lambda''} + \xi_{\lambda\lambda'} \tau_{\mathbf{r},\lambda'}), \tag{2}$$

$$1/\tau_\lambda^0 \equiv \sum_{\lambda'\lambda''}^{+} \Gamma^{+}_{\lambda\lambda'\lambda''} + \sum_{\lambda'\lambda''}^{-} \frac{1}{2} \Gamma^{-}_{\lambda\lambda'\lambda''}. \tag{3}$$

$\Gamma^{\pm}_{\lambda\lambda'\lambda''}$ are proportional to the three-phonon scattering rates, which must satisfy the energy and momentum conservation conditions: $\omega_\lambda \pm \omega_{\lambda'} = \omega_{\lambda''}$ and $\mathbf{q} \pm \mathbf{q}' = \mathbf{q}'' + \mathbf{K}$, where $\mathbf{K}$ is a reciprocal lattice vector, which is zero for momentum-conserving normal processes and nonzero for resistive umklapp processes.[18] Their expressions can be found in Refs. 18 and 16. $\xi_{\lambda\lambda'} \equiv \omega_{\lambda'} v^z_{\lambda'}/\omega_\lambda v^z_\lambda$. The summation is understood as $\sum^{\pm}_{\lambda'\lambda''} F_{\lambda\lambda'\lambda''} \equiv \sum_{\alpha'}\sum_{\alpha''}\int_{BZ} F_{(\alpha,\mathbf{q}),(\alpha',\mathbf{q}'),(\alpha'',\mathbf{q}\pm\mathbf{q}'+\mathbf{K})} d\mathbf{q}'/V_{BZ}$, where V_{BZ} is the "volume" of the Brillouin zone. Here we neglect the scattering due to isotopes, since it is not the focus of the present study.

Equation (1) should be solved in combination with specific boundary condition. All phonons approaching the boundary $\mathbf{r}_B$ are scattered into modes going away from the boundary, and thus the normal component of the velocity v_n changes sign from negative to positive (the direction into the system is taken as positive). Generally the boundary condition reads[19]

$$g_{\mathbf{r}_B,\lambda}(v_n > 0) = \sum_{\alpha'} \int \mathscr{R}(\lambda,\lambda') g_{\mathbf{r}_B,\lambda'}(v'_n < 0) d\mathbf{q}', \quad (4)$$

which represents the steady-state balance condition. The characteristics of the surface are determined by the function $\mathscr{R}(\lambda,\lambda')$, which is the probability of phonons of mode λ being scattered into mode λ'. Phenomenologically a specularity parameter $p(\lambda)$ is usually introduced to simplify the boundary condition. That is to say, a fraction p of the incident phonons are scattered specularly, and the rest are scattered randomly into different directions. The boundary condition then becomes

$$g_{\mathbf{r}_B,\alpha,\mathbf{q}}(v_n > 0) = p g_{\mathbf{r}_B,\alpha,\mathbf{q}'}(v'_n = -v_n), \quad (5)$$

where $\mathbf{q}'$ is simply the reflection of $\mathbf{q}$. For simplicity, we have constrained ourselves to the completely rough boundary condition; that is, $p = 0$. In this case, the boundary condition is very simple: $g_{\mathbf{r}_B,\alpha,\mathbf{q}}(v_n > 0) = 0$.

The PBTE for the bulk materials does not have the last term of Eq. (1), and thus it can be exactly solved iteratively. In the case of NWs, in principle, we can discretize the $\mathbf{r}$ space, and do the iteration for $\tau_{\mathbf{r},\lambda}$ at each $\mathbf{r}$ point. However, in this case, the computational time and computer memory required becomes a serious concern. To overcome this issue, we approximate $\Delta_{\mathbf{r},\lambda}$ by its average value $\bar{\Delta}_\lambda$ over the cross section, which is evaluated using $\bar{\tau}$, the average of $\tau_{\mathbf{r}}$, and we have the formal solution[21]

$$\tau_{\mathbf{r},\lambda} = \tau^0_\lambda (1 + \bar{\Delta}_\lambda)\left\{1 - e^{-|(\mathbf{r}-\mathbf{r}_b)/\tau^0 v_\lambda|} G_{\mathbf{r},\lambda}\right\}, \quad (6)$$

where $\mathbf{r}_b$ is the point on the surface where the phonon of mode λ can reach moving backward from $\mathbf{r}$, and $G_{\mathbf{r},\lambda}$ is determined by the boundary conditions. For completely diffusive boundary conditions, as considered here, $G_{\mathbf{r},\lambda} = 1$. $\bar{\tau}_\lambda$ can thus be obtained as

$$\bar{\tau}_\lambda = \tau^0_\lambda (1 + \bar{\Delta}_\lambda)\left(\frac{1}{S_c}\int_{S_c}\left\{1 - e^{-|(\mathbf{r}-\mathbf{r}_b)/\tau^0 v_\lambda|}\right\} d\mathbf{s}\right), \quad (7)$$

with S_c being the NW cross section. Equation (7) can be solved iteratively starting with the zeroth-order solution

$$\bar{\tau}^{(0)}_\lambda = \tau^0_\lambda \left(\frac{1}{S_c}\int_{S_c}\left\{1 - e^{-|(\mathbf{r}-\mathbf{r}_b)/\tau^0 v_\lambda|}\right\} d\mathbf{s}\right). \quad (8)$$

$\bar{\tau}^{(0)}_\lambda$ is equivalent to the relaxation-time approximation (RTA). The iteration is repeated until the convergence is achieved. In the RTA, $\Delta_{\mathbf{r},\lambda}$ is zero, and Eq. (6) becomes the exact solution. In contrast, the often used Mathiessen rule, which combines anharmonic scattering and Casimir boundary scattering in a simple way, is never exact. This is especially important for a thin film or a 2D ribbon, where a Casimir boundary scattering rate cannot be defined,[20] but the approach in Eq. (6) continues to be valid.

After $\bar{\tau}_\lambda$ is solved, κ can be calculated as[19]

$$\kappa = \frac{1}{k_B T^2}\sum_\alpha \int f_0(f_0+1)(\hbar\omega_\lambda)^2 \left(v^z_\lambda\right)^2 \bar{\tau}_\lambda \frac{d\mathbf{q}}{(2\pi)^3}. \quad (9)$$

The expression of transition probability $\Gamma^{\pm}_{\lambda,\lambda',\lambda''}$ contains a δ function which can be written as $\delta(\omega_\lambda - W)$,[16,18] with $W = \pm\omega_{\lambda'} + \omega_{\lambda''}$. The straightforward way to handle the δ function is to replace it with a Gaussian function[22]

$$g(\omega_\lambda - W) = \frac{1}{\sqrt{\pi}\sigma} e^{-(\omega_\lambda - W)^2/\sigma^2}. \quad (10)$$

As was done in Ref. 23, we use an adaptive broadening parameter σ. σ is chosen to be of the order of ΔW, where ΔW is the spacing of W. ΔW can be estimated as

$$\Delta W = \left|\frac{\partial W}{\partial \mathbf{q}'}\right| |\Delta q'| = |\mathbf{v}_{\lambda'} - \mathbf{v}_{\lambda''}||\Delta q'|, \quad (11)$$

which varies from process to process. $|\Delta q'|$ is simply the spacing of the sampling $\mathbf{q}$ points in the Brillouin zone.

The harmonic and third-order anharmonic interatomic force constants used in this work are calculated from first principles using density functional perturbation theory.[24] The full details of the approach used can be found in Refs. 16 and 24. However, for the benefit of the reader, we note some key elements of the calculations here. These first-principle calculations are performed for the respective bulk systems using a plane-wave pseudopotential method. The electronic exchange and correlation is described using the local-density approximation. The Bachelet-Hamann-Schlüter carbon pseudopotential[25] with a plane-wave energy cutoff of 100 Ry is used for all diamond calculations. Harmonic interatomic force constants are calculated on a $6 \times 6 \times 6$ Monkhorst-Pack q-point mesh and provide phonon dispersions in excellent agreement with experiment for both silicon and diamond. The calculated anharmonic interatomic force constants include interactions up to the seventh nearest neighbors. While the presence of the surfaces will lead to a change in force constants for atoms in this region, we assume this is essentially included in the boundary condition in the diffusive limit. This assumption should be reasonable for the nanowires considered in this work. For small nanowires (2–3 nm or less), a more detailed atomistic examination of the force constants would be required. A $32 \times 32 \times 32$ grid of $\mathbf{q}$ sampling is used to calculate the three-phonon processes for the PBTE calculation in order to achieve good convergence of κ.

III. RESULTS AND DISCUSSION

First we compare the iteratively calculated results with the RTA results. The room temperature κ as a function of

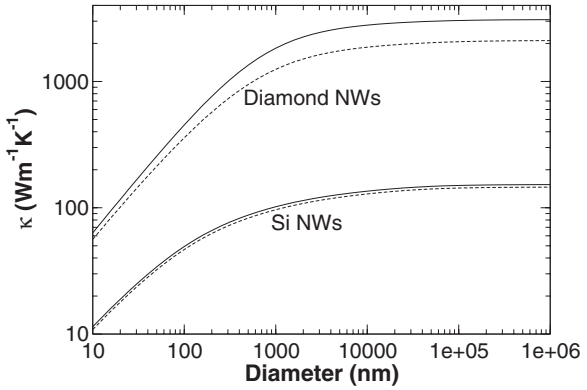

FIG. 1. Comparison of room-temperature thermal conductivities between iteratively calculated results (solid lines) and RTA results (dashed lines) for NWs along [001] growth direction. Upper (lower) curves for diamond (Si) NWs.

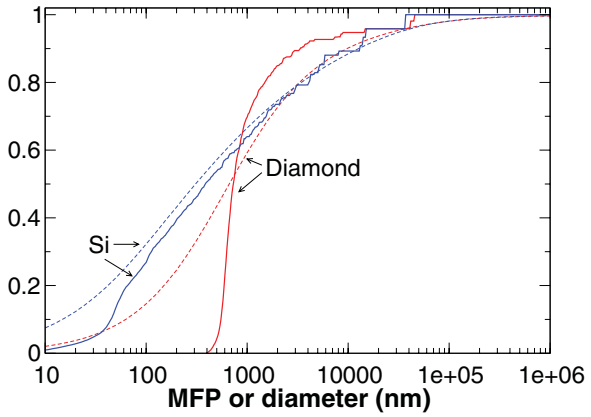

FIG. 2. (Color online) Solid lines: normalized cumulative thermal conductivity of bulk diamond and Si at room temperature, as a function of the mean free path. Dashed lines: room-temperature thermal conductivities of diamond and Si nanowires along [001] growth direction, as a function of diameter, normalized by their corresponding bulk values.

diameter for diamond NWs are plotted in Fig. 1, together with Si NWs for comparison. The iteratively calculated results give the correct bulk value in the large diameter limit. The calculated thermal conductivity approaches the RTA results in the small diameter limit where boundary scattering should dominate over anharmonic phonon-phonon scattering. While the difference between the iteratively calculated κ and the RTA results is almost negligible for Si NWs, it is important for diamond NWs. For example, at 200 nm diameter, the iteratively calculated κ is 33% higher than the RTA value, and it approaches 50% at the bulk limit. If there is some specularity at the surface, the difference is closer to the bulk limit. The iteration procedure removes the contribution of normal three-phonon processes to the thermal resistance, which is included in the RTA. In diamond, the normal processes are important, resulting in a much higher κ than the RTA solution.[16] The difference decreases with decreasing diameter, because anharmonic scattering becomes less important than the boundary scattering. Given that our results match the expected physical trends in the large and small diameter limits, we expect that our results should be in reasonable agreement with the exact solution for the entire diameter range considered here.

It is instructive to take a look at the distribution of phonon mean free paths (MFPs) in the bulk material. We define the MFP of a phonon mode λ as $v_\lambda \tau_\lambda$. A clear view of the MFP distribution is provided by the "cumulative thermal conductivity" κ_l/κ, which represents the fraction of heat carried by phonons with MFPs shorter than or equal to l. It is shown in Fig. 2 for room temperature, where a first striking difference with Si becomes apparent: in bulk diamond, most of the heat is carried by phonons in a narrow range of MFPs, whereas for Si MFPs span a range larger by more than one order of magnitude. In diamond, phonons with 500 nm $< l <$ 3.5 μm account for 80% of the heat, whereas in Si this range becomes 50 nm $< l <$ 13 μm. This difference can be traced to the fact that at room temperature, for Si, the full spectrum of acoustic phonon modes has high occupation, while for diamond only the lowest part of the spectrum has high occupation. Thus, the potential contribution of those shorter MFP phonons in diamond is not present at room temperature.

In a nanosystem one expects that phonons with long MFPs will be blocked by boundaries, thus their contribution to the conductivity would be eliminated. In such a simplified picture one would expect the relative decrease of κ to take place within a narrower range of sizes in diamond as compared to Si. This is indeed the case, as the actual calculation for NWs along [001] growth direction shows, also in Fig. 2. In diamond NWs, κ decreases to about half its bulk value at diameters about 670 nm, as compared to 310 nm for Si NWs. At the same diameter, κ is reduced more significantly in diamond NWs than in Si NWs compared with the bulk value. For instance, κ is reduced to 25% of the bulk value in diamond NWs at 200 nm, compared to 43% in Si NWs. At the point of largest slope in the curve, the change in κ normalized to the bulk value as a function of diameter in diamond NWs is $\sim$1.5 times greater than in Si NWs. All these comparisons indicate that the boundary scattering affects κ more considerably in diamond NWs than in Si NWs at room temperature. From the figure it also becomes clear that the cumulative function is a useful tool for understanding the size behavior, but it cannot be used to predict the actual κ expected in a nanowire. The cumulative and nanowire curves are clearly different. Also, the cumulative curve would predict a markedly faster decrease of κ with decreasing size for Si than diamond for the thicker wires (above 2 μm diameter), but the difference is much less pronounced in the actual nanowire calculation. This is because the effect of the boundaries is not as clear-cut at a certain MFP, but it affects different phonons by a different amount depending on their MFPs as well as the phonon propagation direction with respect to the axis of the wires. This results in an effective spread of the onset of size effects across a large range of lengths, which makes the Si and diamond cases rather close at large diameters. On the contrary, on the small diameter end, the differences are much more marked, and they become manifest in the nanowire case, although not as sharply as the cumulative function would suggest.

Measuring κ as a function of temperature for various diameters is possibly the most direct way to assess the validity

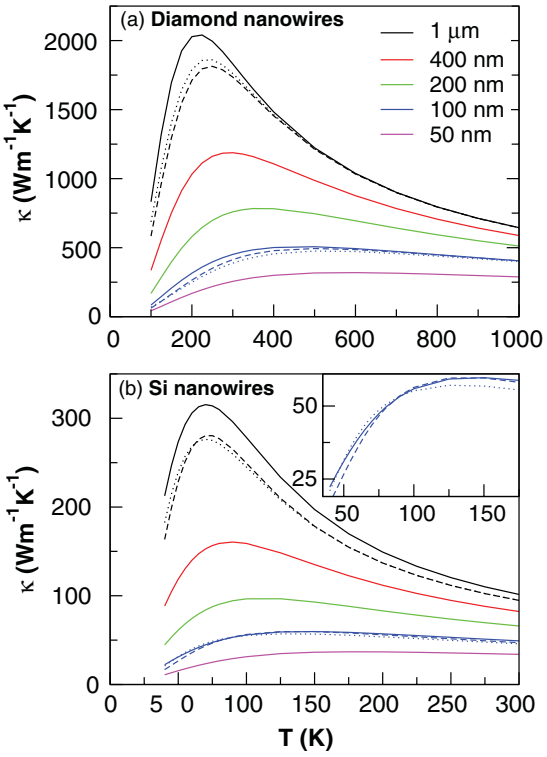

FIG. 3. (Color online) κ versus temperature for (a) diamond NWs and (b) Si NWs along the growth direction [001] (solid lines), [011] (dotted lines), and [111] (dashed lines) for several diameters. The inset shows a zoom-in for 100 nm diameter.

of a calculation. Figure 3(a) shows the predicted results for T in the 100–1000 K range (lower temperatures require a finer grid of $\mathbf{q}$ points which is out of the calculational capability), for the [001] crystallographic direction. No measurement of $\kappa(T)$ on diamond NWs has been yet reported, so these theoretical results still await experimental confirmation. For comparison, the *ab initio* results for Si NWs are also plotted in Fig. 3(b). These are generally larger than the measured values in Ref. 26. Including isotope scattering, a good theoretical fit to the Ref. 26 data has been obtained.[27] However, the isotope scattering rates used ($\tau_i^{-1} = A\omega^4$) in Ref. 27 were ten times too large because A was taken from Ref. 28 which erroneously published a ten times too large value for Si. Using the correct value of A, the reduction of the room-temperature κ of Si NWs is generally less than 7% for all diameters, and κ is still larger than the measured value. For diamond NWs, the reduction of κ due to natural abundance isotope scattering is 12% for 100 nm diameter at room temperature, while the reduction is 30% for bulk diamond.[16] Figure 3 again highlights the large difference between the Si and diamond cases. The size effect at room temperature in diamond NWs is very clear for diameters as large as 400 nm, where a monotonic increase of $\kappa(T)$ is the signature of phonon transport being dominated by boundary scattering. In contrast, a similar size Si nanowire shows a mostly bulklike behavior at room temperature, with the peak $\kappa(T)$ at about 90 K. This has important experimental consequences, meaning that it could be considerably easier to investigate size effects in diamond NWs than in Si, due to the larger sizes involved. In particular, an accurate experimental investigation of diamond NWs might be able to clarify interesting and highly debated phenomena reported on Si NWs, for which experiments are quite involved due to their small diameters.[29]

Up to this point we have only discussed the [001] growth direction. Early experiments on Si rods at low temperature had observed changes as large as 50% depending on orientation.[30,31] Our *ab initio* calculation in Fig. 3 shows that κ of diamond NWs also have a strong orientation dependence. For example, at room temperature, κ for the [001] direction is $\sim$17% larger than the [011] direction at 100 nm diameter, which should be observable in experiments. When the boundary scattering dominates the thermal resistance, as at low temperatures and small diameters, the phonon dispersion itself determines the anisotropy of κ. Considering the linear dispersion at low frequencies, the degree of the κ anisotropy defined as the ratio of κ's along different directions becomes constant at very low temperatures. κ scales linearly with diameter for thin NWs, therefore the degree of the κ anisotropy is also independent of diameter at small diameters. When the temperature and diameter increase, anharmonic scattering starts to play a role in the resistance, and the degree of the κ anisotropy no longer shows a simple relation with the phonon dispersion.

In diamond NWs, calculated results show that the largest conductivity is obtained for the [001] direction, whereas the [011] and [111] directions have smaller conductivities, irrespective of the diameter and the temperature. This indicates that the [001] direction is of the greatest importance in the potential application of diamond NWs in heat management. Our results differ from the calculations in Refs. 32 and 33, which had predicted a larger κ for the [011] direction. However, the calculations in Refs. 32 and 33 are for ultrathin NWs with important quantum confinement effects, so they should not be compared with the ones presented here. On the contrary, the anisotropy of κ in Si NWs shows a more complicated behavior. At 1000 nm diameter, [001] direction has the largest κ, the same as in diamond NWs. However at 100 nm diameter, the highest conductivity can occur in any of the three growth directions, depending on the temperature. We note that the degree of the κ anisotropy in diamond NWs is generally larger than Si NWs for the temperature range involved.

The diamond nanowires whose synthesis is reported in Ref. 1 are encased in carbon nanotubes, although they can be stripped of such cover. If at the contacts the wire is encapsulated in a carbon nanotube, this could in principle add a contact thermal resistance, due to the extra interfaces. However, the answer is not so simple. The conductance of a contact, either phononic or electronic, critically depends on the coupling strength. Weak- and strong-coupling regimes can result in completely opposite physical behaviors. As shown in Ref. 34, a weak coupling requires the contact to be very long, in order to achieve the maximum contact conductance permitted by the quantum limits. On the contrary, a strong coupling quickly reaches a saturated value upon increase of the contact length, but the maximum conductance achievable is typically much less than in the weak-coupling case.

In the case of a nanotube encapsulating the contact part of the wire, the contact between the nanotube and the wire

is probably weak, due to the low reactivity of the graphitic surface. This could be very advantageous, if one can afford making a long contact, since it might allow one to reduce the contact resistance to the lowest possible value. An estimation of the contact strengths and required contact lengths would need a completely different type of calculation, involving Green's function methods, and it is beyond the scope of this paper.

IV. CONCLUSION

We have calculated the thermal conductivity of diamond nanowires beyond the relaxation-time approximation, by using an *ab initio* PBTE calculation. The thermal conductivity of diamond NWs displays unusual properties that differ from those of Si NWs. We have shown that size effects should be more easily observable in diamond NWs than in Si NWs, because κ is more strongly affected at considerably larger diameters and at higher temperatures. We have found that growth direction has an important effect on κ, the [001] direction being the most conductive in diamond NWs, while it is not always the case in Si NWs. Also in contrast with Si, we have shown that normal processes play an important role in diamond NWs, noticeably increasing κ above the RTA values. From the fundamental point of view, these effects imply that an experimental investigation of the thermal conductivity of diamond NWs might be able to clarify the complex nature of the size effects in NWs in a more straightforward way than has been previously possible with Si. From the applications point of view, the ability to use much larger sized diamond NWs that operate at higher temperatures and have faster size variation in κ means that they could play an interesting role as components of thermal management in nanodevices.

ACKNOWLEDGMENTS

We thank C. Jeong and M. Lundstrom for helpful discussions on the cumulative thermal conductivity. We acknowledge N. Vast and F. Mauri for discussions and support from Agence Nationale de la Recherche through project ACCATTONE. L.L. acknowledges support from DARPA. D.A.B. and D.A.S. acknowledge support from NSF under Grant Nos. 1066634 and 1066406.

*wu.li@cea.fr
†natalio.mingo@cea.fr

[1] C.-H. Hsu, S. G. Cloutier, S. Palefsky, and J. Xu, Nano Lett. **10**, 3272 (2010); N. J. Yang, H. Uetsuka, E. Osawa, and C. E. Nebel, *ibid.* **8**, 3572 (2008); H. Masuda, T. Yanagishita, K. Yasui, K. Nishio, I. Yagi, T. N. Rao, and A. Fujishima, Adv. Mater. **13**, 247 (2001); L. T. Sun, J. L. Gong, D. Z. Zhu, Z. Y. Zhu, and S. X. He, *ibid.* **16**, 1849 (2004); I. I. Vlasov, O. I. Lebedev, V. G. Ralchenko, E. Goovaerts, G. Bertoni, G. Van Tendeloo, and V. I. Konov, *ibid.* **19**, 4058 (2007); N. Shang, P. Papakonstantinou, P. Wang, A. Zakharov, U. Palnitkar, I-Nan Lin, M. Chu, and A. Stamboulis, ACS Nano **3**, 1032 (2009).
[2] Y. Chen, D. Li, J. R. Lukes, and A. Majumdar, J. Heat Transfer **127**, 1129 (2005).
[3] N. Mingo, Phys. Rev. B **68**, 113308 (2003).
[4] N. Mingo, L. Yang, D. Li, and A. Majumdar, Nano Lett. **3**, 1713 (2003).
[5] I. Ponomareva, D. Srivastava, and M. Menon, Nano Lett. **7**, 1155 (2007).
[6] T. Markussen, A.-P. Jauho, and M. Brandbyge, Nano Lett. **8**, 3771 (2008).
[7] D. Donadio and G. Galli, Phys. Rev. Lett. **102**, 195901 (2009).
[8] P. Martin, Z. Aksamija, E. Pop, and U. Ravaioli, Phys. Rev. Lett. **102**, 125503 (2009).
[9] P. Martin, Z. Aksamija, E. Pop, and U. Ravaioli, Nano Lett. **10**, 1120 (2010).
[10] C. W. Padgett, O. Shenderova, and D. W. Brenner, Nano Lett. **6**, 1827 (2006).
[11] J. F. Moreland, J. B. Freund, and G. Chen, Nanoscale Microscale Thermophys. Eng. **8**, 61 (2004).
[12] R. E. Peierls, *Quantum Theory of Solids* (Oxford University Press, London, 1955).
[13] M. Omini and A. Sparavigna, Phys. Rev. B **53**, 9064 (1996).
[14] M. Omini and A. Sparavigna, Nuovo Cimento Soc. Ital. Fis., D **19**, 1537 (1997).
[15] D. A. Broido, M. Malorny, G. Birner, N. Mingo, and D. A. Stewart, Appl. Phys. Lett. **91**, 231922 (2007).
[16] A. Ward, D. A. Broido, D. A. Stewart, and G. Deinzer, Phys. Rev. B **80**, 125203 (2009).
[17] A. Kundu, N. Mingo, D. A. Broido, and D. A. Stewart, Phys. Rev. B **84**, 125426 (2011).
[18] L. Lindsay, D. A. Broido, and N. Mingo, Phys. Rev. B **82**, 161402 (2010).
[19] J. M. Ziman, *Electrons and Phonons* (Clarendon Press, London, 1962).
[20] Z. Wang and N. Mingo, Appl. Phys. Lett. **99**, 101903 (2011).
[21] Page 455 in Ref. 19.
[22] X. Tang and J. Dong, Proc. Natl. Acad. Sci. USA **107**, 4539 (2010).
[23] J. R. Yates, X. Wang, D. Vanderbilt, and I. Souza, Phys. Rev. B **75**, 195121 (2007).
[24] G. Deinzer, G. Birner, and D. Strauch, Phys. Rev. B **67**, 144304 (2003).
[25] G. B. Bachelet, D. R. Hamann, and M. Schlüter, Phys. Rev. B **26**, 4199 (1982).
[26] D. Li *et al.*, Appl. Phys. Lett. **83**, 2934 (2003).
[27] Z. Tian, K. Esfarjani, J. Shiomi, A. S. Henry, and G. Chen, Appl. Phys. Lett. **99**, 053122 (2011).
[28] M. G. Holland, Phys. Rev. **132**, 2461 (1963).
[29] R. Chen, A. I. Hochbaum, P. Murphy, J. Moore, P. Yang, and A. Majumdar, Phys. Rev. Lett. **101**, 105501 (2008).
[30] A. K. McCurdy, H. J. Maris, and C. Elbaum, Phys. Rev. B **2**, 4077 (1970).
[31] W. S. Hurst and D. R. Frankl, Phys. Rev. **186**, 801 (1969).
[32] J.-W. Jiang, B.-S. Wang, and J.-S. Wang, Phys. Rev. B **83**, 235432 (2011).
[33] J. Guo, B. Wen, R. Melnik, S. Yao, and T. Li, Physica E **43**, 155 (2010).
[34] N. Mingo and J. Han, Phys. Rev. B **64**, 201401(R) (2001).